

Review

# Recent Advances of Nanomaterials-Based Molecularly Imprinted Electrochemical Sensors

Xinning Dong, Congcong Zhang, Xin Du  and Zhenguo Zhang \*

Shandong Provincial Key Laboratory of Animal Resistance Biology, Key Laboratory of Food Nutrition and Safety, College of Life Sciences, Shandong Normal University, Jinan 250014, China; 201913010337@stu.sdnu.edu.cn (X.D.); zhangcc1026@163.com (C.Z.)

\* Correspondence: xdu@sdnu.edu.cn (X.D.); zhangzg@sdnu.edu.cn (Z.Z.)

**Abstract:** Molecularly imprinted polymer (MIP) is illustrated as an analogue of a natural biological antibody-antigen system. MIP is an appropriate substrate for electrochemical sensors owing to its binding sites, which match the functional groups and spatial structure of the target analytes. However, the irregular shapes and slow electron transfer rate of MIP limit the sensitivity and conductivity of electrochemical sensors. Nanomaterials, famous for their prominent electron transfer capacity and specific surface area, are increasingly employed in modifications of MIP sensors. Staying ahead of traditional electrochemical sensors, nanomaterials-based MIP sensors represent excellent sensing and recognition capability. This review intends to illustrate their advances over the past five years. Current limitations and development prospects are also discussed.

**Keywords:** electrochemical sensor; nanomaterials; molecularly imprinted; polymer



**Citation:** Dong, X.; Zhang, C.; Du, X.; Zhang, Z. Recent Advances of Nanomaterials-Based Molecularly Imprinted Electrochemical Sensors. *Nanomaterials* **2022**, *12*, 1913. <https://doi.org/10.3390/nano12111913>

Academic Editors: Gian Andrea Rizzi and Seong Jung Kwon

Received: 25 April 2022

Accepted: 30 May 2022

Published: 3 June 2022

**Publisher's Note:** MDPI stays neutral with regard to jurisdictional claims in published maps and institutional affiliations.



**Copyright:** © 2022 by the authors. Licensee MDPI, Basel, Switzerland. This article is an open access article distributed under the terms and conditions of the Creative Commons Attribution (CC BY) license (<https://creativecommons.org/licenses/by/4.0/>).

## 1. Introduction

MIP is vividly illustrated as a system of artificial “locks” for “molecular keys”. In this idea, the “key” refers to the target analyte, and its well-matched “locks” are made of MIP. This analogue of a natural biological antibody-antigen system contributes to the selectivity of molecularly imprinted electrochemical sensors [1]. MIP can be utilized to coat the electrode surface to prepare MIP electrochemical sensors. There have been many methods exploited to prepare MIP [2], including layer-by-layer self-assembly, in situ chemical polymerization, sol-gel, and electro-polymerization. Electro-polymerization is an electrochemical method for preparation of conductive or nonconductive thin MIP film onto the transducer surface [3]. It is the generation technology with most potential for a multitude of reasons. First of all, the electrode surface can be coated by a uniform MIP membrane via just one step. Secondly, its thickness and shape can be regulated by parameters such as voltage and current, which provides sensor preparation with high reproducibility [4]. In addition, MIP sensors can operate in body fluid environments, allowing preparatory processes to take place in an aqueous solution [5].

The basic principle was illustrated in the schematic diagram of Figure 1. Firstly, nanomaterials were designed and synthesized, then modified on the polished electrode surface to enhance its conductivity and specific surface area. Secondly, MIP was electro-polymerized on it, and then template molecules were removed by solvent elution, leaving 3D cavities that could specifically match template molecules [6]. It was reported that the voltammetric sensors were the most common type; in this approach, electric signals would show a weakening trend after analytes' recombination as the charge transfer between the electrode and redox probes was blocked. The content of analytes could be easily detected through quantitative analysis by linearizing the conversion values.

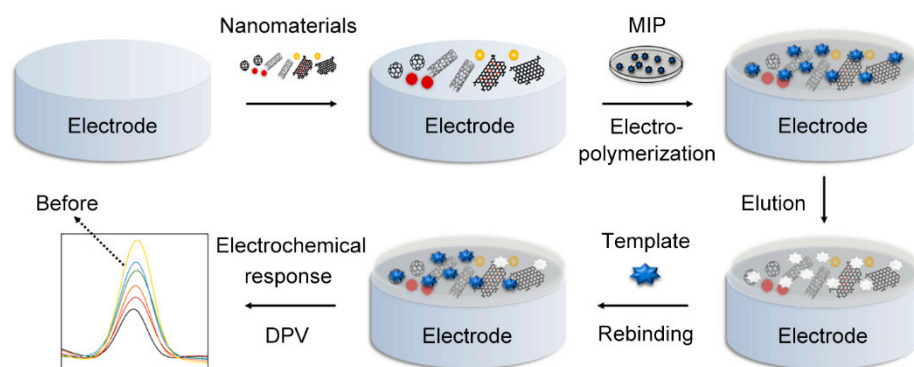


**Figure 1.** The construction and detection process of an MIP sensor.

MIP sensors were designed for the detection of chemical compounds, proteins, cells [7,8], or other substances [9]. MIP-based sensors have many advantages. They can identify and recombine targets with high specificity, and are much cheaper than natural antibodies. Since they appeared, MIP sensors have been extensively applied in medical diagnosis [10,11], food safety [12–14], and environmental monitoring fields [10,15]. However, there are still some restrictions, such as uneven polymerization and low electric conductivity, which could be nicely solved by the attachment of nanomaterials [16].

## 2. Applications of Nanomaterials in MIP Sensors

Nanomaterials refer to materials with at least one dimension in nanoscale (0.1~100 nm) or that are composed of nanoscale units in three-dimensional (3D) space. Owing to their desirable properties, such as surface and interface effects, macroscopic quantum tunnel effect and quantum size effect, nanomaterials show great potential to improve the performance of overall electrochemical oxidation/reduction and alleviate the drawbacks concerning interference of other substances. In addition, sensors will be easily miniaturized and their adsorption capacity can be enhanced [17] with nanomaterials as the supporting materials [13].

### 2.1. Carbon Nanomaterials-Based MIP Sensors

The ratio of  $sp/sp^2/sp^3$  hybridizations determines the formation of 3D carbon nanomaterials, 2D carbon sheets (graphene-based nanomaterials), 1D and hollow nanomaterials (carbon nanotubes), and 0D nanomaterials (carbon quantum dots) [18,19]. Besides the morphological structures, the ratio also decides their electrochemical properties [20].

#### 2.1.1. Carbon Nanotube-Based MIP Sensors

Formed by wrapped graphene, carbon nanotubes (CNTs) are mainly appearing as single-walled CNTs (SWCNTs) and multi-walled CNTs (MWCNTs). Having distinct thickness and metallic/semiconducting properties, both of them possess delicately adjustable electrochemical characteristics [21], such as rapid electron transfer capacity, large specific surface area, and easy functionalization [22,23]. Several studies demonstrated that CNTs could act as “electronic wire” between the surface of electrodes and the redox center of a protein, which significantly accelerated the direct electron-transfer reaction. Shumyantseva et al. [23] prepared a MWCNTs/MIP sensor via electro-polymerization of *o*-phenylenediamine (*o*-PD) and template myoglobin (Mb) on the MWCNTs’ modified screen-printed electrodes (SPE) surface. It was demonstrated to offer greater accuracy in undiluted plasma samples. Hussein et al. [24] developed a sensor by electro-polymerizing MIP on CNTs/ $WO_3$  modified SPE to detect SARS-CoV-2 particles. All preparation and detection processes were shown in the Figure 2. Its limit of detection (LOD) was  $57 \text{ pg mL}^{-1}$ , and the electron transfer velocity was more rapid than that of other nanomaterial-based sensors.

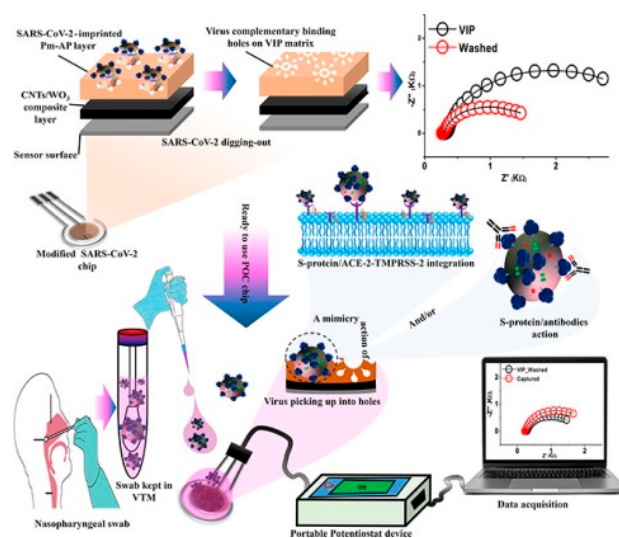


**Figure 2.** The construction and detection process of MIP sensors [24].

Zhang et al. [16] polymerized a MIP film onto the vinyl group functionalized MWCNTs, which had better thermal stability. The hottest modification method was to treat MWCNTs with strong oxidants such as nitric acid to generate COOH. This carboxylated process could produce a large number of imprinted sites and oxygen-containing functional groups, which aided in adsorption, electron transport [20], and water dispersion of CNTs. Wu et al. [25] carboxylated MWCNTs with strong acids and then dropped them onto a polished glassy carbon electrode (GCE) surface to obtain MWCNTs/GCE. Subsequently, chitosan (CS) and tryptophan (Trp) mixture was applied to modify the GCE surface to form a MIP chitosan film. Characterized by cyclic voltammetry (CV), the oxidation current signal of MWCNTs/MIP/GCE was 2.1 times higher than that of MIP/GCE. Ma et al. [26] employed a composite of MWCNTs/CS and acrylamide (AAM) to a modified electrode. CS was not only used to provide amino groups for adsorption of glutaraldehyde (GA) and HIV-p24, but acted as a conductive bridge for electron transfer. Yu et al. [27] utilized MIP/SWCNTs-COOH/CS to modify GCE for semicarbazide (SEM) detection. Owing to the hydrogen bonding between CS and SWCNTs-COOH, the CS solubilization of CNTs was facilitated. Shaabani et al. [28] reported a sensitive sol-gel MIP sensor for urine naloxone (NLX) detection. NLX was added into initial sol and magnetically stirred for an hour to build the imprinted sol. After that, pyrrole (Py) was added to fabricate the Py@solgelMIP/fMWCNTs/ITO sensor. Because MIP and sol-gel were not electroconductive, nanomaterials were introduced. Carboxylated MWCNTs were evenly dispersed and made into a 3D reticular formation to increase current transport and binding sites. Akhoundian et al. [29] prepared a carbon nanocomposite paste electrode for ultra-trace trimipramine (TRI) analysis. MIP with a selective site was synthesized via precipitation polymerization by monomer vinyl benzene (VB) and methacrylic acid (MAA). The sensor could determine the concentration of TRI in a broad range, without pretreatment of serum samples and concerns about the interference effect caused by other substances.

The analytes, functional monomers, electrode modification, linear range, and LOD of CNT-based MIP sensors were listed in Table 1. Sensor properties are affected by the length and diameter of CNTs, so the modification processes should be fully characterized by a scanning electron microscope (SEM). There are still some implications that need to be taken into account, such as toxicity [30], biocompatibility, and the long-term effect on the ecosystem of CNTs [22].

**Table 1.** CNT-based molecularly imprinted sensors.

Analyte	Functional Monomers	Electrode Modification	Linear Range	LOD	Refs
Mb	o-PD	MIP/MWCNTs	$1 \times 10^{-11} \sim 5 \times 10^{-10}$ , $5 \times 10^{-10} \sim 5 \times 10^{-8}$ M	$1 \times 10^{-11}$ M	[23]
SARS-CoV-2	m-AP	MIP/CNTs/WO <sub>3</sub>	7~320 pg mL <sup>-1</sup>	57 pg mL <sup>-1</sup>	[24]
Trp	CS	MIP/MWCNTs	$2 \times 10^{-7} \sim 1 \times 10^{-5}$ , $1 \times 10^{-5} \sim 1 \times 10^{-4}$ M	$1 \times 10^{-9}$ M	[25]
HIV-p24	AAM	MIPs/MWCNTs/CS	$1 \times 10^{-4} \sim 2$ ng cm <sup>-3</sup>	0.083 pg cm <sup>-3</sup>	[26]
SEM	o-PD	MIP/SWNTs-COOH/CS	0.040~7.6 ng mL <sup>-1</sup>	0.025 ng mL <sup>-1</sup>	[27]
NLX	TEPS/Py	Py@solgelMIP/ fMWCNTs	$0 \sim 1.2 \times 10^{-5}$ M	$2 \times 10^{-8}$ M	[28]
TRI	MAA/VB	MIP/MWCNTs	$1 \times 10^{-10} \sim 2.5 \times 10^{-8}$ M	$4.52 \times 10^{-11}$ M	[29]

### 2.1.2. Graphene-Based MIP Sensors

In 2004, researchers discovered a method to prepare single-layer planar graphene sheets of atomic thickness [31]. Graphene is described as a large polycyclic aromatic with 2D sheets consisting of sp<sup>2</sup> bonded carbon atoms. The surface area of graphene sheets is so large [32] that it offers numerous active sites for further modification [33]. Its superior conductivity was calculated as 64 mS cm<sup>-1</sup>, which was about sixty times stronger than that of SWCNTs. Liu et al. [34] developed a novel sensor by electro-polymerization of epigallocatechin-gallate (EGCG) and beta-cyclodextrins on electrodes with graphene oxide (GO) modification. This MIP sensor presented extraordinary advantages over conventional approaches because of the one-step preparation by CV scans without elution reagent. Liu et al. [17] successfully developed a GO-sheets modified MIP sensor for the detection of testosterone. The EIS response indicated the enhancement of sensitivity. Similar sensors could be further expanded to other endogenous substances. Several graphene-based MIP sensors were described in Table 2.

Moreira et al. [35] used reduced graphene oxide (rGO) to modify the GCE surface, and then electro-polymerized the MIP membrane by CV with phenol as the functional monomer. As a poor conductor, GO needed to be transformed to rGO [36], which contained fewer oxygen functional groups [37]. rGO@MIP preserved the merits of graphene@MIP and showed excellent conductivity and adsorption capacity [38]. The LOD of this sensor was seven times lower than that of high-performance liquid chromatography. Meanwhile, the morphological characterization revealed a rise in the surface roughness of rGO-based electrodes, which was conducive to the adhesion of MIP film and enhanced the imprinted cavities number up to 15 times. In their another research report, phenol was replaced with phenylboric acid (PBA) for selective detection of fructose [39]. PBA, which could form reversible borate esters through covalent interactions, was the suitable functional monomer for sugar recognition. Maryam Mostafavi et al. [40] synthesized sensors by rGO and polyaniline for the determination of diclofenac (DCF). It was shown via Fourier-transform infrared spectroscopy (FT-IR) and SEM imaging that the nano-layered structure of rGO made the electrolyte able to diffuse into the intervals of the sheets, thereby enhancing its conductive characteristics.

It was critical to make GO evenly distributed and fixed on the GCE surface [41], and dopamine (DA) had been discovered as an outstanding surface-adherent material. Bai et al. [42] fabricated an advanced MIP sensor by coating DA@graphene (DGr) and electro-polymerizing Py on the electrode. Polypyrrole (PPy) film fixed DGr. With the enhanced current response, the sensor could specifically recognize olaquinox (OLA) from its analogues, and its analysis of fish and feedstuffs showed a satisfactory result.

**Table 2.** Graphene-based molecularly imprinted sensors.

Analyte	Functional Monomers	Electrode Modification	Linear Range	LOD	Refs
EGCG	beta-CD	MIP/GO	$3 \times 10^{-8} \sim 1 \times 10^{-5}$ M	$8.78 \times 10^{-9}$ M	[34]
Testosterone	o-PD	MIP/GO	$1 \times 10^{-15} \sim 1 \times 10^{-6}$ M	$4.0 \times 10^{-16}$ M	[17]
D-xylose	Phenol	MIP/rGO	$1.0 \times 10^{-13} \sim 1.0 \times 10^{-10}$ M	$8.0 \times 10^{-14}$ M	[35]
Fructose	PBA	MIP/rGO	$1.0 \times 10^{-14} \sim 1.0 \times 10^{-11}$ M	$1.1 \times 10^{-14}$ M	[39]
DCF	Polyaniline	MIP/rGO	5~80 mg L <sup>-1</sup>	1.1 mg L <sup>-1</sup>	[40]
OLA	Py	MIP/DGr	$5 \times 10^{-8} \sim 5 \times 10^{-7}$ M	$7.5 \times 10^{-9}$ M	[42]

### 2.1.3. Carbon Quantum Dot-Based MIP Sensors

Carbon quantum dots (CQDs), consisting of carbon dots (CDs) and graphene quantum dots (GQDs), are 0D photoluminescent materials at the forefront of carbon nanomaterials research [43]. Derived from functionalized graphene, GQDs are several graphene sheets with lateral sizes below 100 nm. Owing to their outstanding electronic properties and low toxicity, CQDs have become suitable alternatives to conventional semiconductor QDs and carbon materials [44]. Although CQDs remain in the development stage, they are promising modifiers due to their simple synthesis and versatility. Applications of GQDs in MIP electrochemical sensors far exceed those of CDs [45,46].

Zheng et al. [47] proposed a novel MIP sensor with CDs and CS to improve its electron transportability. According to the study of Rao et al. [48], using Py as functional monomer, they electro-polymerized MIP film onto an electrode, which was modified by hollow nickel nanosphere-decorated GQDs. Based on the interaction between functional groups on GQDs and bisphenol S (BPS), functionalized GQDs could significantly improve the sensor detection velocity for BPS, which exhibited a LOD of  $3 \times 10^{-8}$  M under optimized conditions. Yao et al. [49] fabricated an electroconductive layer that was made of AgNPs and three-doped CQDs (B, N, F-CQDs). The sensitivity of the electrode was markedly improved by the synergy between them, which made it relevant for constant testing instead of chromatographic analysis. A PPy MIP membrane was further modified on the electrode. With a LOD of  $1.12 \times 10^{-8}$  M, the sensor could realize trace-level survey of analyte in plastic product samples.

Based on their unique fluorescence property, CQD-based fluorescence MIP sensors are an inspiring method. Jalili et al. [50] constructed a ratiometric fluorescent sensor with CDs as fluorophores. In this method, blue emissive CDs (B-CDs) were incorporated into silica-spheres, and yellow-emissive CDs (Y-CDs) were embedded in the MIP. When the 3D cavities on MIP film recombined with the analyte, the fluorescence color changed from the yellow to blue due to the fluorescence quenching of Y-CDs. The resulting ratios of fluorescence intensities at 560 nm and 440 nm could be used for trace level detection of penicillin-G in milk samples. Traditional QDs were generally extracted from lead, cadmium, and silicon, etc. Therefore, they were poisonous and deleterious to the environment. CDs have no relation to heavy metals and have excellent biocompatibility [51]. In practical applications, the main challenge is to seek innovative synthesis methods for high-quality CQDs with considerable yield [44].

## 2.2. Metal Nanoparticles-Based MIP Sensors

### 2.2.1. Gold Nanoparticles-Based MIP Sensors

Inert metal nanoparticles have been broadly used to assess biological analytes, as their integration of aptamers and MIP can greatly improve the electrochemical performance of sensors [52,53]. Gold nanoparticles (AuNPs), with high biocompatibility, are essential to the sensor surface functionalization. They also provide the possibility of rapid electron transport between the electrode and the redox probe to enhance the resistance value changes. Zhang et al. [54] modified a gold electrode (GE) with AuNPs, polythionine-methylene blue (PTH-MB), and MIP in sequential order. Its current response was three

times stronger than that of unmodified GE. The biosensor showed two oxidative peaks at  $-0.22$  V and  $0.20$  V referred to PTH-MB and  $[\text{Fe}(\text{CN})_6]^{3-}/4-$ , thus the amount of human serum albumin (HSA) in urine could be quantified by calculating the totality of double signals. In the investigation of Sehit [55], MIP/AuNP sensors had good specificity for glucose in human serum, whereas other sensors without AuNPs could not detect even the highest concentration of the research range. Yu et al. [56] constructed a MIP film on the electrode surface after AuNPs modification, which was generated by electro-polymerization of DA, polythymine aptamers, and melamine (MEL).

Motia et al. [57] functionalized the Au-SPE with AuNPs and electro-polymerized acrylamide/methylenebisacrylamide (AAM/NNMBA) on it to design an electrochemical MIP sensor for glycerol determination. The electro-kinetic analysis illustrated that the blend of AuNPs and polymer complex had a better sensitivity. In 2021, they [58] prepared another sensor for butylated hydroxyanisole (BHA) recognition, through electro-polymerization of AuNPs and CS. To demonstrate the role of AuNPs, they contrasted the sensitivity of sensors before and after modification, and then concluded that the sensitivity of (MIP-AuNPs)/SPCE was 12 times higher.

Recently, AuNPs have been incorporated into the modification of electrodes, acting as supporting materials for MIP. To obtain a high ratio of imprinted sites, AuNPs can be made into novel shapes with a larger surface area, and considering their good biocompatibility, they have already been applied in determination of organic and inorganic small molecules, such as protein or alcohol. Several AuNPs-based MIP sensors were listed in Table 3.

### 2.2.2. Silver Nanoparticles-Based MIP Sensors

Silver is emerging as the best conductor among metals. Many properties of silver nanoparticles (AgNPs) have been widely acknowledged, such as large specific surface area, excellent biocompatibility, antimicrobial characteristics, and catalytic performance [59]. However, their applications in MIP sensors are slightly limited because of poor oxidative stability [60].

Nezhadali et al. [61] constructed a bi-layer of AgNPs and PPy for mebeverine (MEB). In this sensor, Py was electro-polymerized onto the electrode surface and then AgNPs were added by potentiostatic electrodeposition, which exhibited a brilliant electrocatalytic effect and amplified the electrochemical response. Noble metals had a surface plasmon resonance (SPR) effect and a AgNPs layer would have dense plasmonic hot spots to achieve ultrasensitive analysis. Zhao et al. [62] formed a sandwich structure of 3D silver dendrites (SD)/MIP/AgNPs by a paper-based surface-enhanced Raman scattering (SERS) amplified approach. SD in conjunction with AgNPs had constructed double Ag layers, and realized multistage enhancement of the SERS signal on the basis of the superposition of their electric and magnetic fields. The contribution processes of the sensor were illustrated in the Figure 3.

### 2.2.3. Platinum Nanoparticles-Based MIP Sensors

Platinum nanoparticles (PtNPs) possess brilliant electrocatalytic activity and have been applied to MIP electrochemical sensing. For example, Xu et al. [63] firstly incorporated UiO-66 with PtNPs to detect phosalone (PAS). Using N-[3-(trimethoxysilyl) propyl] aniline (PAPTMS) and 3-aminobenzenboronic acid (APBA) as functional monomer, active sites abounded on Pt-doped UiO-66 octahedrons. In tests of environmental samples, the sensors showed an ultra-low LOD ( $0.078$  nM). Liu et al. [64] constructed a novel sensor by electrodepositing a dual-monomer MIP film on the electrode with Pt/Co<sub>3</sub>O<sub>4</sub> nanoparticles modification. These transition metal oxides supported by noble-metal catalysts had a good catalytic activity and large surface area to enhance the detection sensitivity of the sensor. Under optimal conditions, this sensor exhibited a satisfactory anti-interference ability for chlorpromazine (CPZ) detection.

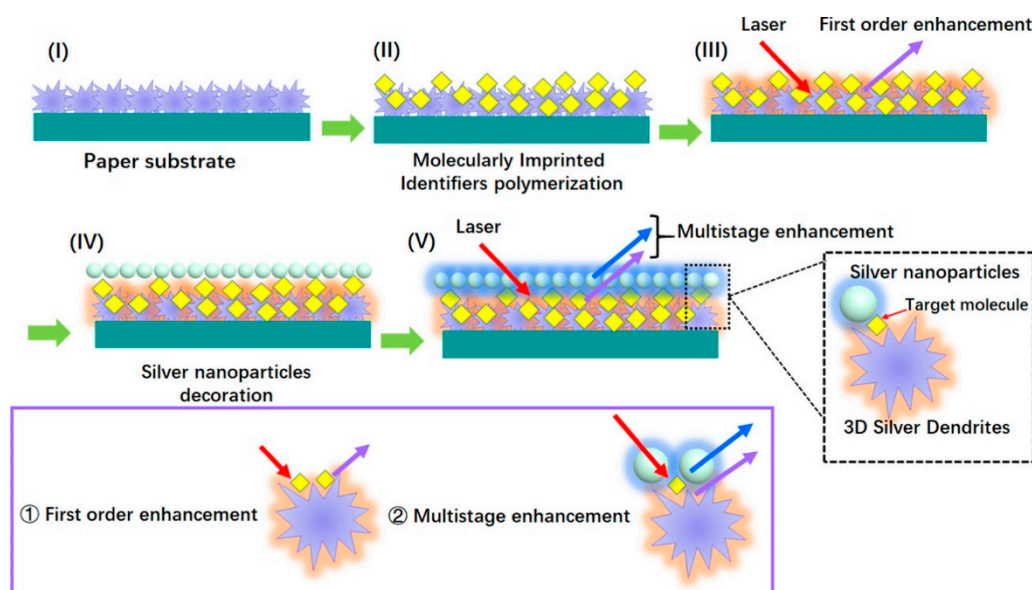


**Figure 3.** The 3D silver dendrites (SD)/MIP/AgNPs sensor was contributed through following steps [62]. (I) SD were grown on the paper substrate. (II) SD were coated by MIP film. (III) When laser light was incident, the first order enhancement generated but was not strong enough. (IV) The AgNPs layer was further decorated on it. (V) Multistage enhancement effect was produced by double Ag layers.

**Table 3.** Metal nanoparticles-based molecularly imprinted sensors.

Analyte	Functional Monomers	Electrode Modification	Linear Range	LOD	Refs
HSA	o-PD/HQ	MIP/AuNPs/PTH-MB	$1 \times 10^{-10} \sim 1 \times 10^{-4} \text{ g L}^{-1}$	$3 \times 10^{-11} \text{ g L}^{-1}$	[54]
Glucose	o-PD	MIP/AuNPs	$1.25 \times 10^{-9} \sim 2.56 \times 10^{-6} \text{ M}$	$1.25 \times 10^{-9} \text{ M}$	[55]
MEL	DA/poly T	MIP/AuNPs	$1 \times 10^{-12} \sim 1 \times 10^{-4} \text{ M}$	$6.7 \times 10^{-13} \text{ M}$	[56]
Glycerol	Acrylamide	MIP/AuNPs	$20 \sim 227.81 \text{ } \mu\text{g mL}^{-1}$	$0.001 \text{ } \mu\text{g mL}^{-1}$	[57]
BHA	CS	MIP/AuNPs	$0.01 \sim 20 \text{ } \mu\text{g mL}^{-1}$	$0.001 \text{ } \mu\text{g mL}^{-1}$	[58]
MEB	PPy	MIP/AgNPs	$1 \times 10^{-8} \sim 1 \times 10^{-6}$ , $1 \times 10^{-5} \sim 1 \times 10^{-3} \text{ M}$	$8.6 \times 10^{-9} \text{ M}$	[61]
IMI	EMIs	SD/MIP/AuNPs	$0.2 \sim 800 \text{ ng mL}^{-1}$	$0.028 \text{ ng mL}^{-1}$	[62]
PSA	PAPTMS/APBA	MIP/PtNPs	$5 \times 10^{-10} \sim 2 \times 10^{-5} \text{ M}$	$7.8 \times 10^{-11} \text{ M}$	[63]
Cocaine	PABA	MIP/PdNPs	$1 \times 10^{-4} \sim 5 \times 10^{-4} \text{ M}$	$5 \times 10^{-5} \text{ M}$	[65]
CHO	PDA	MIP/Pt/AuNPs	$1 \times 10^{-12} \sim 5 \times 10^{-11} \text{ M}$	$2 \times 10^{-13} \text{ M}$	[66]
6-MP	N-AAsp	MIP/N-HCNS@PdNPs	$0.8 \sim 70.748 \text{ ng mL}^{-1}$	$0.11 \sim 0.22 \text{ ng mL}^{-1}$	[67]

#### 2.2.4. Palladium Nanoparticles-Based MIP Sensors

Palladium nanoparticles (PdNPs) are emerging noble metal nanomaterials, with outstanding electrical characteristics, oxidation resistance, and catalytic performance. Compared to other precious metal nanoparticles, such as gold, PdNPs are much cheaper and more easily available. Florea et al. [65] electrodeposited PdNPs on graphene-functionalized SPE (GPH-SPE). The deposition was conducive to the uniform distribution of p-aminobenzoic acid (PABA) and expanded the number of imprinted sites. In comparison with the single metal NPs, applications of bimetallic alloy NPs seemed to be much wider, and bimetallic Au/PdNPs were one of the most preferred alloys. Jalalvand et al. [66] electrodeposited Au/PdNPs and used polydopamine (PDA) as a functional monomer to establish a novel MIP sensor for cholestanol (CHO) test. Kumar et al. [67] decorated N-doped carbon nanospheres (N-CNS) with PdNPs and subsequently etched silica moieties to make them

hollow (N-HCNS). N-acryloyl derivative of aspartic acid (N-AAsp), the appropriate functional monomer with carboxylic functional groups, has been applied to anchoring metal ions. Via electrostatic interactions, N-HCNS@Pd-MIP was adsorbed on the ionic liquid (IL) modified pencil graphite electrode. As a result of 6-mercaptopurine (6-MP) detection, the N-HCNS@Pd-MIP modified sensor obtained twice the heterogeneous rate constant, 3.5 times the diffusion coefficient, and 10 times electrical conductivity, compared to that of the N-CNS@Pd-MIP.

### 2.3. Metal Derivative Nanomaterials-Based MIP Sensors

#### 2.3.1. Metal Oxide Nanomaterials-Based MIP Sensors

Various metal oxide nanoparticles are composed of iron, zinc, copper, titanium, manganese, and so on [68]. Their unique properties, such as nontoxicity, piezoelectricity, and biocompatibility, have widened their applications in MIP electrochemical sensors [69]. For instance, Wang et al. [70] electrodeposited ZnO nanotubes (ZNTs) onto fluorine-doped tin oxide (FTO) glass to be high-surface 3D supports for MIP arrays. For electrodeposition of MIP, CV was performed in Py aqueous solution, and then in phosphate buffer solution to extract embedded DA. In this case, most imprinted sites were located at both internal and external surfaces of ZNTs, which shortened the charge transport pathway. Therefore, the sensor showed two dynamic linear ranges to DA, which were 0.02~5  $\mu\text{M}$  and 10~800  $\mu\text{M}$ . This preparation strategy could be further desired to be universal to imprint biomolecules. Yu et al. [71] added Py and nonylphenol into the  $\text{TiO}_2$  nanoparticles' ( $\text{TiO}_2\text{NPs}$ ) dispersion. Then, NP-PPy@ $\text{TiO}_2$ MIP suspension was dropped and dried on the cleaned GCE surface to form MIP.  $\text{TiO}_2\text{NPs}$ , used as carriers, were capable of extending the detection range of p-nonylphenol (p-NP) to  $1 \times 10^{-8}$ ~ $8 \times 10^{-5}$  M.

#### 2.3.2. Metal Sulfide Nanomaterials-Based MIP Sensors

Transition metal dichalcogenides (TMDs) are known as graphene analogues, which are made by stacking transition metal and sulfur sheets through van der Waals forces [72]. Molybdenum disulfide ( $\text{MoS}_2$ ) is a typical example.

$\text{MoS}_2$  has attracted widespread attention in MIP fields such as hydrogen catalysis and storage because it shortens the electron transfer distance [73]. Significantly, with relatively low conductivity, it needs to accommodate additional nanomaterials to be operational [74]. Axin Liang et al. [75] modified GCE with highly conductive  $\text{MoS}_2$ @N-GQDs-IL to magnify electrochemical signals for human immunoglobulin G (IgG).  $\text{MoS}_2$  was functionalized with nitrogen-doped GQDs (N-GQDs). Their integration with IL afforded an effective sensing platform, which contributed to the powerful electrostatic chemical interactions between  $\text{MoS}_2$ @N-GQDs and IL.  $\text{CuFe}_2\text{O}_4$  was used as the carrier to prepare the MIP. At the optimal conditions, the reaction was curtailed within 8 min with perfect accuracy and stability.

### 2.4. Nanocomposite-Based MIP Sensors

Nanocomposite, formed by nanomaterials combined with other organic or inorganic functional substances, is appropriate for functional utilization. Nanocomposite not only integrates the advantages of a single nanomaterial but also gains the synergistic effect of multiple components [53]. Wang et al. [76] modified AuNPs on cMWCNTs/GCE through chronoamperometry in  $\text{HAuCl}_4$ . On this foundation, MIP film was electro-polymerized using o-PD as the monomer. This sensor finally had high sensitivity and could offer a 2.7 nM LOD for OLA. Liu et al. [77] designed a flexible electrochemical (EC) sensor with MIP and nanocomposite for urea detection in human sweat. As shown in the Figure 4, after the CNTs were loaded on AuNTs film, 3,4-ethylenedioxythiophene (EDOT) monomer was subsequently electro-polymerized. This strategy paved the way for epidermal noninvasive tests of other substances.

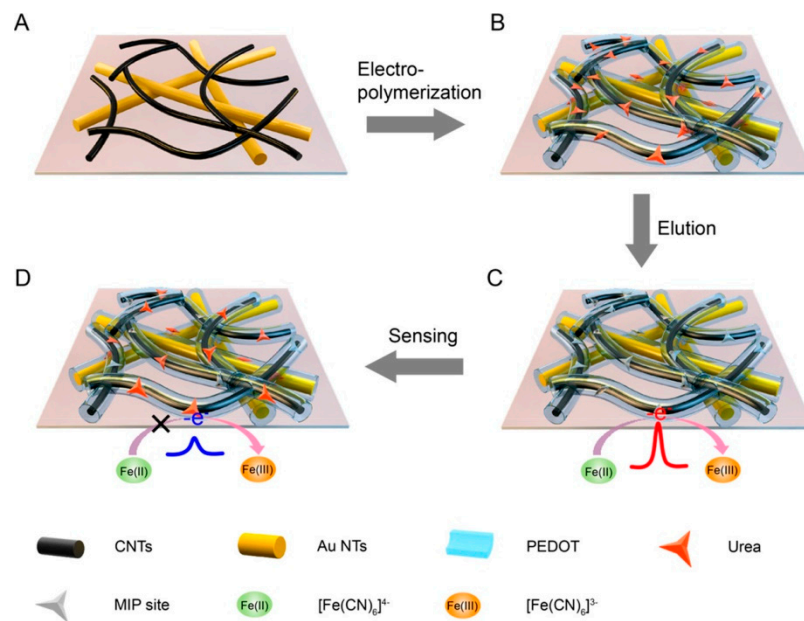


**Figure 4.** Fabrication of the MIP/C-AuNTs/PDMS EC sensor [77].

Chitosan (CS), with lots of amino groups and hydroxyl groups, is a biocompatible biopolymer with good film-forming ability and high mechanical strength [78]. Lian et al. [79] increased the electrochemical response through the synergistic effects of graphene-MWCNTs and CS-AgNPs. As the most important index of electrochemical sensors, it was essential to broaden the active area of the electrode surface and accelerate electrolyte diffusion. Guo et al. [80] modified the electrode with nanocomposite to acquire distinct electric signals. Homogeneously distributed CS-CDs and AuNPs ameliorated the bare GCE surface with more roughness. Moreover, introducing AuNPs for building the Au-S bond was an essential step to connect with the functional monomer  $\rho$ -Aminothiophenol ( $\rho$ -ATP). In comparison with conventional methods such as chromatographies and immunoassays, this sensor had higher sensitivity, faster processing speed, lower sample consumption, and lower cost.

rGO was usually compounded with AuNPs, and the nanocomposite had a faster electron transport speed and higher catalytic activity [81]. Beluomini et al. [82] electrodeposited rGO and AuNPs on GCE to develop a sensor for D-mannitol (D-M) determination in sugarcane vinasse. MIP was electro-polymerized on the AuNP/rGO-GCE by CV in acetate buffer solution containing D-M and o-PD. Its LOD was  $7.7 \times 10^{-13}$  M, and its selectivity to D-M was about six times as high as that of other reported electrochemical sensors. In a separate study, Zhang et al. [83] mixed the rGO with CS solution at a volume ratio of 1:1, and added the AuNPs for ultrasonic stirring to acquire AuNPs@rGO. Then, Py was electro-polymerized on AuNPs@rGO modified electrode. According to the report, this novel sensor could determine serum amyloid A (MAA) more rapidly, sensitively, and cheaply compared to the enzyme-linked immunosorbent assay (ELISA) method, which is the only present technique to monitor MAA. Yang et al. [4] developed a MIP-AuNPs-PDA-DGr/GCE sensor for ultra-trace monitoring of cholesterol (CHO). In this process, PDA was implemented not only to disperse graphene but also to produce a multifunctional platform on graphene to steady AuNPs and MIP films. Wrapped by PDA, AuNPs could grow into versatile Au microflowers. Au-S and intermolecular forces between PDA and functional monomers guaranteed the stable immobilization of MIP film. Wang et al. [84] successfully synthesized a polyethyleneimine (PEI)-rGO-gold nanoclusters (Au-NCs)@MIP sensor. Both rGO and AuNPs in nanocomposite could diminish the electrode surface resistance, making recognition of  $\beta$ -lactoglobulin ( $\beta$ -LG) faster and more accurate. Choline chloride (ChCl) and acrylic acid (AA) were used for hydrothermal synthesis of MIP. In actual samples tests, the LOD was  $109 \text{ mg mL}^{-1}$ , much lower than the ELISA of  $20 \text{ mg mL}^{-1}$ .

We summarized attributes of several nanocomposites-based MIP sensors in Table 4. According to the characteristics of target analytes, it is promising to comprehensively use different nanomaterials with different functions and adopt various modification methods for preparing ideal sensors.

**Table 4.** Nanocomposite-based molecularly imprinted sensors.

Analyte	Functional Monomers	Electrode Modification	Linear Range	LOD	Refs
OLA	o-PD	MIP/AuNPs/cMWCNTs	$1 \times 10^{-8} \sim 2 \times 10^{-7}$ M	$2.7 \times 10^{-9}$ M	[76]
Urea	EDOT	MIP/C-AuNTs	$1 \times 10^{-3} \sim 0.1$ M	$1 \times 10^{-4}$ M	[77]
Patulin	$\rho$ -ATP	MIP/AuNPs/CS-CDs	$1 \times 10^{-12} \sim 1 \times 10^{-9}$ M	$7.57 \times 10^{-13}$ M	[80]
D-M	o-PD	MIP/AuNPs/rGO	$1 \times 10^{-12} \sim 2 \times 10^{-11}$ , $2 \times 10^{-11} \sim 3 \times 10^{-10}$ M	$7.7 \times 10^{-13}$ M	[82]
MAA	Py	MIP/AuNPs@rGO	$0.01 \sim 200$ ng mL <sup>-1</sup>	$5$ pg mL <sup>-1</sup>	[83]
CHO	ATP	MIP/AuNPs/PDA/DGr	$1 \times 10^{-18} \sim 1 \times 10^{-13}$ M	$3.3 \times 10^{-19}$ M	[4]
$\beta$ -LAC	ChCl/AA	PEI-rGO-Au-NCs@MIP	$1 \times 10^{-9} \sim 1 \times 10^{-4}$ mg mL <sup>-1</sup>	$1 \times 10^{-9}$ mg mL <sup>-1</sup>	[84]

### 3. Conclusions and Prospects

Nanomaterials play an irreplaceable role in the advances of electrochemical sensors, which tremendously decrease their LODs to the femto level. In this review, we summed up the present advances of nanomaterials-based electrochemical MIP sensors. Most notably, nanocomposite is gradually becoming the mainstream in application of MIP electrochemical sensors, and portable, sensitive, and low-cost nanomaterials-based MIP electrochemical sensing devices will be more prevalent in the foreseeable future.

Further investigations of nanomaterials in MIP sensors are expected to be carried out focusing on three aspects. Firstly, according to the chemical structure of target analytes, it is significant to innovate new functional monomers with high specificity toward them. Secondly, we should pay more attention to the combination forms of nanomaterials and MIP in sensors to obtain a better overall performance. Last but not least, more effective fixation methods of modifiers in electrochemical MIP sensors are supposed to be exploited, as the leakage or exfoliation of modifiers can reduce the sensing surface sites and the electronic conductivity of the sensors.

**Author Contributions:** Conceptualization, X.D. (Xinning Dong) and Z.Z.; writing—original draft preparation, X.D. (Xinning Dong); writing—review and editing, C.Z., X.D. (Xin Du) and Z.Z.; funding acquisition, X.D. (Xin Du) and Z.Z. All authors have read and agreed to the published version of the manuscript.

**Funding:** The financial supports from National Natural Science Foundation of China (Grant nos. 32170734 and 32170921) and the Young Talent of Lifting engineering for Science and Technology in Shandong, China (SDAST2021qt07) are acknowledged.

**Conflicts of Interest:** The authors declare no competing interests.

### References

1. BelBruno, J.J. Molecularly Imprinted Polymers. *Chem. Rev.* **2019**, *119*, 94–119. [[CrossRef](#)] [[PubMed](#)]
2. Gui, R.; Jin, H.; Guo, H.; Wang, Z. Recent Advances and Future Prospects in Molecularly Imprinted Polymers-Based Electrochemical Biosensors. *Biosens. Bioelectron.* **2018**, *100*, 56–70. [[CrossRef](#)] [[PubMed](#)]
3. Sharma, P.S.; Pietrzyk-Le, A.; D'Souza, F.; Kutner, W. Electrochemically Synthesized Polymers in Molecular Imprinting for Chemical Sensing. *Anal. Bioanal. Chem.* **2012**, *402*, 3177–3204. [[CrossRef](#)] [[PubMed](#)]
4. Yang, H.; Li, L.; Ding, Y.; Ye, D.; Wang, Y.; Cui, S.; Liao, L. Molecularly Imprinted Electrochemical Sensor Based on Bioinspired Au Microflowers for Ultra-Trace Cholesterol Assay. *Biosens. Bioelectron.* **2017**, *92*, 748–754. [[CrossRef](#)] [[PubMed](#)]
5. Blanco-López, M.C.; Gutiérrez-Fernández, S.; Lobo-Castañón, M.J.; Miranda-Ordieres, A.J.; Tuñón-Blanco, P. Electrochemical Sensing with Electrodes Modified with Molecularly Imprinted Polymer Films. *Anal. Bioanal. Chem.* **2004**, *378*, 1922–1928. [[CrossRef](#)]

6. Karimian, N.; Stortini, A.M.; Moretto, L.M.; Costantino, C.; Bogialli, S.; Ugo, P. Electrochemosensor for Trace Analysis of Perfluorooctanesulfonate in Water Based on a Molecularly Imprinted Poly(o-Phenylenediamine) Polymer. *ACS Sens.* **2018**, *3*, 1291–1298. [[CrossRef](#)]
7. Dar, K.K.; Shao, S.; Tan, T.; Lv, Y. Molecularly Imprinted Polymers for the Selective Recognition of Microorganisms. *Biotechnol. Adv.* **2020**, *45*, 107640. [[CrossRef](#)]
8. Piletsky, S.; Canfarotta, F.; Poma, A.; Bossi, A.M.; Piletsky, S. Molecularly Imprinted Polymers for Cell Recognition. *Trends Biotechnol.* **2020**, *38*, 368–387. [[CrossRef](#)]
9. Ayankojo, A.G.; Reut, J.; Ciocan, V.; Öpik, A.; Syrtiski, V. Molecularly Imprinted Polymer-Based Sensor for Electrochemical Detection of Erythromycin. *Talanta* **2020**, *209*, 120502. [[CrossRef](#)]
10. Kadhem, A.J.; Gentile, G.J.; Fidalgo de Cortalezzi, M.M. Molecularly Imprinted Polymers (MIPs) in Sensors for Environmental and Biomedical Applications: A Review. *Molecules* **2021**, *26*, 6233. [[CrossRef](#)]
11. Saylan, Y.; Akgönüllü, S.; Yavuz, H.; Ünal, S.; Denizli, A. Molecularly Imprinted Polymer Based Sensors for Medical Applications. *Sensors* **2019**, *19*, E1279. [[CrossRef](#)] [[PubMed](#)]
12. Elfadil, D.; Lamaoui, A.; Della Pelle, F.; Amine, A.; Compagnone, D. Molecularly Imprinted Polymers Combined with Electrochemical Sensors for Food Contaminants Analysis. *Molecules* **2021**, *26*, 4607. [[CrossRef](#)] [[PubMed](#)]
13. Cao, Y.; Feng, T.; Xu, J.; Xue, C. Recent Advances of Molecularly Imprinted Polymer-Based Sensors in the Detection of Food Safety Hazard Factors. *Biosens. Bioelectron.* **2019**, *141*, 111447. [[CrossRef](#)] [[PubMed](#)]
14. Sundhoro, M.; Agnihotra, S.R.; Amberger, B.; Augustus, K.; Khan, N.D.; Barnes, A.; BelBruno, J.; Mendecki, L. An Electrochemical Molecularly Imprinted Polymer Sensor for Rapid and Selective Food Allergen Detection. *Food Chem.* **2021**, *344*, 128648. [[CrossRef](#)] [[PubMed](#)]
15. Rebelo, P.; Costa-Rama, E.; Seguro, I.; Pacheco, J.G.; Nouws, H.P.A.; Cordeiro, M.N.D.S.; Delerue-Matos, C. Molecularly Imprinted Polymer-Based Electrochemical Sensors for Environmental Analysis. *Biosens. Bioelectron.* **2021**, *172*, 112719. [[CrossRef](#)]
16. Zhang, D.; Yu, D.; Zhao, W.; Yang, Q.; Kajiura, H.; Li, Y.; Zhou, T.; Shi, G. A Molecularly Imprinted Polymer Based on Functionalized Multiwalled Carbon Nanotubes for the Electrochemical Detection of Parathion-Methyl. *Analyst* **2012**, *137*, 2629–2636. [[CrossRef](#)]
17. Liu, W.; Ma, Y.; Sun, G.; Wang, S.; Deng, J.; Wei, H. Molecularly Imprinted Polymers on Graphene Oxide Surface for EIS Sensing of Testosterone. *Biosens. Bioelectron.* **2017**, *92*, 305–312. [[CrossRef](#)]
18. Slepčková Kasálková, N.; Slepčička, P.; Švorčík, V. Carbon Nanostructures, Nanolayers, and Their Composites. *Nanomaterials* **2021**, *11*, 2368. [[CrossRef](#)]
19. Loh, K.P.; Ho, D.; Chiu, G.N.C.; Leong, D.T.; Pastorin, G.; Chow, E.K.-H. Clinical Applications of Carbon Nanomaterials in Diagnostics and Therapy. *Adv. Mater.* **2018**, *30*, e1802368. [[CrossRef](#)]
20. Yang, C.; Denno, M.E.; Pyakurel, P.; Venton, B.J. Recent Trends in Carbon Nanomaterial-Based Electrochemical Sensors for Biomolecules: A Review. *Anal. Chim. Acta* **2015**, *887*, 17–37. [[CrossRef](#)]
21. McCreery, R.L. Advanced Carbon Electrode Materials for Molecular Electrochemistry. *Chem. Rev.* **2008**, *108*, 2646–2687. [[CrossRef](#)] [[PubMed](#)]
22. De Menezes, B.R.C.; Rodrigues, K.F.; da Fonseca, B.C.S.; Ribas, R.G.; do Montanheiro, T.L.A.; Thim, G.P. Recent Advances in the Use of Carbon Nanotubes as Smart Biomaterials. *J. Mater. Chem. B* **2019**, *7*, 1343–1360. [[CrossRef](#)] [[PubMed](#)]
23. Shumyantseva, V.V.; Bulko, T.V.; Sigolaeva, L.V.; Kuzikov, A.V.; Pogodin, P.V.; Archakov, A.I. Molecular Imprinting Coupled with Electrochemical Analysis for Plasma Samples Classification in Acute Myocardial Infarction Diagnostic. *Biosens. Bioelectron.* **2018**, *99*, 216–222. [[CrossRef](#)] [[PubMed](#)]
24. Hussein, H.A.; Kandeil, A.; Gomaa, M.; Mohamed El Nashar, R.; El-Sherbiny, I.M.; Hassan, R.Y.A. SARS-CoV-2-Impedimetric Biosensor: Virus-Imprinted Chips for Early and Rapid Diagnosis. *ACS Sens.* **2021**, *6*, 4098–4107. [[CrossRef](#)]
25. Wu, Y.; Deng, P.; Tian, Y.; Ding, Z.; Li, G.; Liu, J.; Zuberi, Z.; He, Q. Rapid Recognition and Determination of Tryptophan by Carbon Nanotubes and Molecularly Imprinted Polymer-Modified Glassy Carbon Electrode. *Bioelectrochemistry* **2020**, *131*, 107393. [[CrossRef](#)]
26. Ma, Y.; Shen, X.-L.; Zeng, Q.; Wang, H.-S.; Wang, L.-S. A Multi-Walled Carbon Nanotubes Based Molecularly Imprinted Polymers Electrochemical Sensor for the Sensitive Determination of HIV-P24. *Talanta* **2017**, *164*, 121–127. [[CrossRef](#)]
27. Yu, W.; Tang, Y.; Sang, Y.; Liu, W.; Wang, S.; Wang, X. Preparation of a Carboxylated Single-Walled Carbon-Nanotube-Chitosan Functional Layer and Its Application to a Molecularly Imprinted Electrochemical Sensor to Quantify Semicarbazide. *Food Chem.* **2020**, *333*, 127524. [[CrossRef](#)]
28. Shaabani, N.; Chan, N.W.C.; Jemere, A.B. A Molecularly Imprinted Sol-Gel Electrochemical Sensor for Naloxone Determination. *Nanomaterials* **2021**, *11*, 631. [[CrossRef](#)]
29. Akhoundian, M.; Alizadeh, T.; Ganjali, M.R.; Rafiei, F. A New Carbon Paste Electrode Modified with MWCNTs and Nano-Structured Molecularly Imprinted Polymer for Ultratrace Determination of Trimipramine: The Crucial Effect of Electrode Components Mixing on Its Performance. *Biosens. Bioelectron.* **2018**, *111*, 27–33. [[CrossRef](#)]
30. Yuan, X.; Zhang, X.; Sun, L.; Wei, Y.; Wei, X. Cellular Toxicity and Immunological Effects of Carbon-Based Nanomaterials. *Part. Fibre Toxicol.* **2019**, *16*, 18. [[CrossRef](#)]
31. Novoselov, K.S.; Geim, A.K.; Morozov, S.V.; Jiang, D.; Zhang, Y.; Dubonos, S.V.; Grigorieva, I.V.; Firsov, A.A. Electric Field Effect in Atomically Thin Carbon Films. *Science* **2004**, *306*, 666–669. [[CrossRef](#)] [[PubMed](#)]

32. Stoller, M.D.; Park, S.; Zhu, Y.; An, J.; Ruoff, R.S. Graphene-Based Ultracapacitors. *Nano Lett.* **2008**, *8*, 3498–3502. [[CrossRef](#)] [[PubMed](#)]
33. Liu, C.; Alwarappan, S.; Chen, Z.; Kong, X.; Li, C.-Z. Membraneless Enzymatic Biofuel Cells Based on Graphene Nanosheets. *Biosens. Bioelectron.* **2010**, *25*, 1829–1833. [[CrossRef](#)] [[PubMed](#)]
34. Liu, Y.; Zhu, L.; Hu, Y.; Peng, X.; Du, J. A Novel Electrochemical Sensor Based on a Molecularly Imprinted Polymer for the Determination of Epigallocatechin Gallate. *Food Chem.* **2017**, *221*, 1128–1134. [[CrossRef](#)] [[PubMed](#)]
35. Pompeu Prado Moreira, L.F.; Buffon, E.; Stradiotto, N.R. Electrochemical Sensor Based on Reduced Graphene Oxide and Molecularly Imprinted Poly(Phenol) for d-Xylose Determination. *Talanta* **2020**, *208*, 120379. [[CrossRef](#)]
36. Pumera, M. Graphene-Based Nanomaterials and Their Electrochemistry. *Chem. Soc. Rev.* **2010**, *39*, 4146–4157. [[CrossRef](#)]
37. Wu, S.; He, Q.; Tan, C.; Wang, Y.; Zhang, H. Graphene-Based Electrochemical Sensors. *Small* **2013**, *9*, 1160–1172. [[CrossRef](#)]
38. Liu, B.; Lian, H.; Chen, L.; Wei, X.; Sun, X. Differential Potential Ratiometric Sensing Platform for Enantio-recognition of Chiral Drugs. *Anal. Biochem.* **2019**, *574*, 39–45. [[CrossRef](#)]
39. Moreira, L.F.P.P.; Buffon, E.; de Sá, A.C.; Stradiotto, N.R. Fructose Determination in Fruit Juices Using an Electrosynthesized Molecularly Imprinted Polymer on Reduced Graphene Oxide Modified Electrode. *Food Chem.* **2021**, *352*, 129430. [[CrossRef](#)]
40. Mostafavi, M.; Yafthian, M.R.; Piri, F.; Shayani-Jam, H. A New Diclofenac Molecularly Imprinted Electrochemical Sensor Based upon a Polyaniline/Reduced Graphene Oxide Nano-Composite. *Biosens. Bioelectron.* **2018**, *122*, 160–167. [[CrossRef](#)]
41. Babamiri, B.; Salimi, A.; Hallaj, R.; Hasanzadeh, M. Nickel Nanoclusters as a Novel Emitter for Molecularly Imprinted Electrochemiluminescence Based Sensor toward Nanomolar Detection of Creatinine. *Biosens. Bioelectron.* **2018**, *107*, 272–279. [[CrossRef](#)] [[PubMed](#)]
42. Bai, X.; Zhang, B.; Liu, M.; Hu, X.; Fang, G.; Wang, S. Molecularly Imprinted Electrochemical Sensor Based on Polypyrrole/Dopamine@graphene Incorporated with Surface Molecularly Imprinted Polymers Thin Film for Recognition of Olaquinox. *Bioelectrochemistry* **2020**, *132*, 107398. [[CrossRef](#)] [[PubMed](#)]
43. Molaei, M.J. A Review on Nanostructured Carbon Quantum Dots and Their Applications in Biotechnology, Sensors, and Chemiluminescence. *Talanta* **2019**, *196*, 456–478. [[CrossRef](#)] [[PubMed](#)]
44. Campuzano, S.; Yáñez-Sedeño, P.; Pingarrón, J.M. Carbon Dots and Graphene Quantum Dots in Electrochemical Biosensing. *Nanomaterials* **2019**, *9*, 634. [[CrossRef](#)] [[PubMed](#)]
45. Mansuriya, B.D.; Altintas, Z. Graphene Quantum Dot-Based Electrochemical Immunosensors for Biomedical Applications. *Materials* **2019**, *13*, 96. [[CrossRef](#)] [[PubMed](#)]
46. Gupta, S.; Smith, T.; Banaszak, A.; Boeckl, J. Graphene Quantum Dots Electrochemistry and Sensitive Electrocatalytic Glucose Sensor Development. *Nanomaterials* **2017**, *7*, 301. [[CrossRef](#)] [[PubMed](#)]
47. Zheng, W.; Wu, H.; Jiang, Y.; Xu, J.; Li, X.; Zhang, W.; Qiu, F. A Molecularly-Imprinted-Electrochemical-Sensor Modified with Nano-Carbon-Dots with High Sensitivity and Selectivity for Rapid Determination of Glucose. *Anal. Biochem.* **2018**, *555*, 42–49. [[CrossRef](#)]
48. Rao, H.; Zhao, X.; Liu, X.; Zhong, J.; Zhang, Z.; Zou, P.; Jiang, Y.; Wang, X.; Wang, Y. A Novel Molecularly Imprinted Electrochemical Sensor Based on Graphene Quantum Dots Coated on Hollow Nickel Nanospheres with High Sensitivity and Selectivity for the Rapid Determination of Bisphenol S. *Biosens. Bioelectron.* **2018**, *100*, 341–347. [[CrossRef](#)]
49. Yao, J.; Chen, M.; Li, N.; Liu, C.; Yang, M. Experimental and Theoretical Studies of a Novel Electrochemical Sensor Based on Molecularly Imprinted Polymer and B, N, F-CQDs/AgNPs for Enhanced Specific Identification and Dual Signal Amplification in Highly Selective and Ultra-Trace Bisphenol S Determination in Plastic Products. *Anal. Chim. Acta* **2019**, *1066*, 36–48. [[CrossRef](#)]
50. Jalili, R.; Khataee, A.; Rashidi, M.-R.; Razmjou, A. Detection of Penicillin G Residues in Milk Based on Dual-Emission Carbon Dots and Molecularly Imprinted Polymers. *Food Chem* **2020**, *314*, 126172. [[CrossRef](#)]
51. Mansuriya, B.D.; Altintas, Z. Applications of Graphene Quantum Dots in Biomedical Sensors. *Sensors* **2020**, *20*, 1072. [[CrossRef](#)] [[PubMed](#)]
52. Draz, M.S.; Shafiee, H. Applications of Gold Nanoparticles in Virus Detection. *Theranostics* **2018**, *8*, 1985–2017. [[CrossRef](#)]
53. Tajik, S.; Beitollahi, H.; Nejad, F.G.; Zhang, K.; Le, Q.V.; Jang, H.W.; Kim, S.Y.; Shokouhimehr, M. Recent Advances in Electrochemical Sensors and Biosensors for Detecting Bisphenol A. *Sensors* **2020**, *20*, 3364. [[CrossRef](#)]
54. Zhang, G.; Yu, Y.; Guo, M.; Lin, B.; Zhang, L. A Sensitive Determination of Albumin in Urine by Molecularly Imprinted Electrochemical Biosensor Based on Dual-Signal Strategy. *Sens. Actuators B Chem.* **2019**, *288*, 564–570. [[CrossRef](#)]
55. Sehit, E.; Drzazgowska, J.; Buchenau, D.; Yesildag, C.; Lensen, M.; Altintas, Z. Ultrasensitive Nonenzymatic Electrochemical Glucose Sensor Based on Gold Nanoparticles and Molecularly Imprinted Polymers. *Biosens. Bioelectron.* **2020**, *165*, 112432. [[CrossRef](#)] [[PubMed](#)]
56. Yu, C.; Li, L.; Ding, Y.; Liu, H.; Cui, H.; Zhang, F.; Lin, J.; Duan, Y. A Sensitive Molecularly Imprinted Electrochemical Aptasensor for Highly Specific Determination of Melamine. *Food Chem.* **2021**, *363*, 130202. [[CrossRef](#)]
57. Motia, S.; Bouchikhi, B.; Llobet, E.; El Bari, N. Synthesis and Characterization of a Highly Sensitive and Selective Electrochemical Sensor Based on Molecularly Imprinted Polymer with Gold Nanoparticles Modified Screen-Printed Electrode for Glycerol Determination in Wastewater. *Talanta* **2020**, *216*, 120953. [[CrossRef](#)] [[PubMed](#)]
58. Motia, S.; Bouchikhi, B.; El Bari, N. An Electrochemical Molecularly Imprinted Sensor Based on Chitosan Capped with Gold Nanoparticles and Its Application for Highly Sensitive Butylated Hydroxyanisole Analysis in Foodstuff Products. *Talanta* **2021**, *223*, 121689. [[CrossRef](#)]

59. Zhao, Q.; Zhao, M.; Qiu, J.; Lai, W.-Y.; Pang, H.; Huang, W. One Dimensional Silver-Based Nanomaterials: Preparations and Electrochemical Applications. *Small* **2017**, *13*, 1701091. [[CrossRef](#)]
60. Lee, S.H.; Jun, B.-H. Silver Nanoparticles: Synthesis and Application for Nanomedicine. *Int. J. Mol. Sci.* **2019**, *20*, 865. [[CrossRef](#)]
61. Nezhadali, A.; Bonakdar, G.A. Multivariate Optimization of Mebeverine Analysis Using Molecularly Imprinted Polymer Electrochemical Sensor Based on Silver Nanoparticles. *J. Food Drug Anal.* **2019**, *27*, 305–314. [[CrossRef](#)] [[PubMed](#)]
62. Zhao, P.; Liu, H.; Zhang, L.; Zhu, P.; Ge, S.; Yu, J. Paper-Based SERS Sensing Platform Based on 3D Silver Dendrites and Molecularly Imprinted Identifier Sandwich Hybrid for Neonicotinoid Quantification. *ACS Appl. Mater. Interfaces* **2020**, *12*, 8845–8854. [[CrossRef](#)] [[PubMed](#)]
63. Xu, L.; Li, J.; Zhang, J.; Sun, J.; Gan, T.; Liu, Y. A Disposable Molecularly Imprinted Electrochemical Sensor for the Ultra-Trace Detection of the Organophosphorus Insecticide Phosalone Employing Monodisperse Pt-Doped UiO-66 for Signal Amplification. *Analyst* **2020**, *145*, 3245–3256. [[CrossRef](#)] [[PubMed](#)]
64. Liu, Y.; Hu, X.; Xia, Y.; Zhao, F.; Zeng, B. A Novel Ratiometric Electrochemical Sensor Based on Dual-Monomer Molecularly Imprinted Polymer and Pt/Co<sub>3</sub>O<sub>4</sub> for Sensitive Detection of Chlorpromazine Hydrochloride. *Anal. Chim. Acta* **2022**, *1190*, 339245. [[CrossRef](#)]
65. Florea, A.; Cowen, T.; Piletsky, S.; De Wael, K. Electrochemical Sensing of Cocaine in Real Samples Based on Electrodeposited Biomimetic Affinity Ligands. *Analyst* **2019**, *144*, 4639–4646. [[CrossRef](#)]
66. Jalalvand, A.R.; Zangeneh, M.M.; Jalili, F.; Soleimani, S.; Diaz-Cruz, J.M. An Elegant Technology for Ultrasensitive Impedimetric and Voltammetric Determination of Cholesterol Based on a Novel Molecularly Imprinted Electrochemical Sensor. *Chem. Phys. Lipids* **2020**, *229*, 104895. [[CrossRef](#)]
67. Kumar, A.; Pathak, P.K.; Prasad, B.B. Electrocatalytic Imprinted Polymer of N-Doped Hollow Carbon Nanosphere-Palladium Nanocomposite for Ultratrace Detection of Anticancer Drug 6-Mercaptopurine. *ACS Appl. Mater. Interfaces* **2019**, *11*, 16065–16074. [[CrossRef](#)]
68. George, J.M.; Antony, A.; Mathew, B. Metal Oxide Nanoparticles in Electrochemical Sensing and Biosensing: A Review. *Microchim. Acta* **2018**, *185*, 358. [[CrossRef](#)]
69. Shetti, N.P.; Bukkitgar, S.D.; Reddy, K.R.; Reddy, C.V.; Aminabhavi, T.M. ZnO-Based Nanostructured Electrodes for Electrochemical Sensors and Biosensors in Biomedical Applications. *Biosens. Bioelectron.* **2019**, *141*, 111417. [[CrossRef](#)]
70. Wang, H.-H.; Chen, X.-J.; Li, W.-T.; Zhou, W.-H.; Guo, X.-C.; Kang, W.-Y.; Kou, D.-X.; Zhou, Z.-J.; Meng, Y.-N.; Tian, Q.-W.; et al. ZnO Nanotubes Supported Molecularly Imprinted Polymers Arrays as Sensing Materials for Electrochemical Detection of Dopamine. *Talanta* **2018**, *176*, 573–581. [[CrossRef](#)]
71. Yu, M.; Wu, L.; Miao, J.; Wei, W.; Liu, A.; Liu, S. Titanium Dioxide and Polypyrrole Molecularly Imprinted Polymer Nanocomposites Based Electrochemical Sensor for Highly Selective Detection of P-Nonylphenol. *Anal. Chim. Acta* **2019**, *1080*, 84–94. [[CrossRef](#)] [[PubMed](#)]
72. Kudr, J.; Adam, V.; Zitka, O. Fabrication of Graphene/Molybdenum Disulfide Composites and Their Usage as Actuators for Electrochemical Sensors and Biosensors. *Molecules* **2019**, *24*, 3374. [[CrossRef](#)] [[PubMed](#)]
73. Zhang, A.; Li, A.; Zhao, W.; Liu, J. Recent Advances in Functional Polymer Decorated Two-Dimensional Transition-Metal Dichalcogenides Nanomaterials for Chemo-Photothermal Therapy. *Chemistry* **2018**, *24*, 4215–4227. [[CrossRef](#)] [[PubMed](#)]
74. Huang, H.; Wang, M.; Wang, Y.; Li, X.; Niu, Z.; Wang, X.; Song, J. Electrochemical Determination of 2,4-Dichlorophenol by Using a Glassy Carbon Electrode Modified with Molybdenum Disulfide, Ionic Liquid and Gold/Silver Nanorods. *Microchim. Acta* **2018**, *185*, 292. [[CrossRef](#)]
75. Axin Liang, A.; Huipeng Hou, B.; Shanshan Tang, C.; Liquan Sun, D.; Aiqin Luo, E. An Advanced Molecularly Imprinted Electrochemical Sensor for the Highly Sensitive and Selective Detection and Determination of Human IgG. *Bioelectrochemistry* **2021**, *137*, 107671. [[CrossRef](#)]
76. Wang, H.; Yao, S.; Liu, Y.; Wei, S.; Su, J.; Hu, G. Molecularly Imprinted Electrochemical Sensor Based on Au Nanoparticles in Carboxylated Multi-Walled Carbon Nanotubes for Sensitive Determination of Olaquinox in Food and Feedstuffs. *Biosens. Bioelectron.* **2017**, *87*, 417–421. [[CrossRef](#)]
77. Liu, Y.-L.; Liu, R.; Qin, Y.; Qiu, Q.-F.; Chen, Z.; Cheng, S.-B.; Huang, W.-H. Flexible Electrochemical Urea Sensor Based on Surface Molecularly Imprinted Nanotubes for Detection of Human Sweat. *Anal. Chem.* **2018**, *90*, 13081–13087. [[CrossRef](#)]
78. Deng, P.; Xu, Z.; Kuang, Y. Electrochemical Determination of Bisphenol A in Plastic Bottled Drinking Water and Canned Beverages Using a Molecularly Imprinted Chitosan-Graphene Composite Film Modified Electrode. *Food Chem.* **2014**, *157*, 490–497. [[CrossRef](#)]
79. Lian, W.; Liu, S.; Yu, J.; Li, J.; Cui, M.; Xu, W.; Huang, J. Electrochemical Sensor Using Neomycin-Imprinted Film as Recognition Element Based on Chitosan-Silver Nanoparticles/Graphene-Multiwalled Carbon Nanotubes Composites Modified Electrode. *Biosens. Bioelectron.* **2013**, *44*, 70–76. [[CrossRef](#)]
80. Guo, W.; Pi, F.; Zhang, H.; Sun, J.; Zhang, Y.; Sun, X. A Novel Molecularly Imprinted Electrochemical Sensor Modified with Carbon Dots, Chitosan, Gold Nanoparticles for the Determination of Patulin. *Biosens. Bioelectron.* **2017**, *98*, 299–304. [[CrossRef](#)]
81. Ma, X.; Li, X.; Zhang, W.; Meng, F.; Wang, X.; Qin, Y.; Zhang, M. Carbon-Based Nanocomposite Smart Sensors for the Rapid Detection of Mycotoxins. *Nanomaterials* **2021**, *11*, 2851. [[CrossRef](#)] [[PubMed](#)]
82. Beluomini, M.A.; da Silva, J.L.; Sedenho, G.C.; Stradiotto, N.R. D-Mannitol Sensor Based on Molecularly Imprinted Polymer on Electrode Modified with Reduced Graphene Oxide Decorated with Gold Nanoparticles. *Talanta* **2017**, *165*, 231–239. [[CrossRef](#)] [[PubMed](#)]

83. Zhang, Z.; Chen, S.; Ren, J.; Han, F.; Yu, X.; Tang, F.; Xue, F.; Chen, W.; Yang, J.; Jiang, Y.; et al. Facile Construction of a Molecularly Imprinted Polymer-Based Electrochemical Sensor for the Detection of Milk Amyloid A. *Microchim. Acta* **2020**, *187*, 642. [[CrossRef](#)] [[PubMed](#)]
84. Wang, B.; Hong, J.; Liu, C.; Zhu, L.; Jiang, L. An Electrochemical Molecularly Imprinted Polymer Sensor for Rapid  $\beta$ -Lactoglobulin Detection. *Sensors* **2021**, *21*, 8240. [[CrossRef](#)] [[PubMed](#)]